# Stress optic modulator using thin-film PZT for LIDAR applications

F. Casset, M. Colin, D. Fowler, B. Desloges, S. Malhouitre, T. Hilt, G. Le Rhun, C. Dieppedale, O. Pollet, W. Rabaud

# Stress optic modulator using thin-film PZT for LIDAR applications

F. Casset, D. Fowler, B. Desloges, S. Malhouitre, T. Hilt, G. Le Rhun, C. Dieppedale, O. Pollet, W. Rabaud, M. Colin
[1]Univ. Grenoble Alpes, CEA, LETI, 38000 Grenoble, France
fabrice.casset@cea.fr

***Abstract*—This paper presents the development of a stress optic modulator which can be implemented in an optical sensor system such as LIDAR. In LIDAR, an Optical Phased Array (OPA), consisting of several optical waveguides, can be used to steer the direction of light beams. The beam steering can be achieved using phase shifters where the delay for different optical waveguides is changed via the waveguide optical index by applying a mechanical stress using thin-film piezoelectric actuators. Finite Element Method (FEM) simulation was used to design the stress optic modulator and demonstrators were built on 200 mm silicon wafers and thin-film $Pb(Zr_{0.52},Ti_{0.48})O_3$ (PZT) material. Electrical and optical measurements were performed on our stress optic modulator and show the efficiency of the PZT phase shifter as being in the range of $V\pi L\pi$ = 20-26 V.cm, with an estimated energy dissipation of 800 nW per π phase shift. The proposed method suggests an alternative path to low power and high frequency solid-state LIDAR optical sensor systems.**

***Keywords—Stress optic modulator; LIDAR; piezoelectric; PZT; optical sensor system***

## I. INTRODUCTION

Light Detection And Ranging (LIDAR) systems [1, 2] are increasingly studied for the autonomous vehicles [3, 4, 5], which has to have 3D mapping capabilities in order to detect obstacles. LIDAR is similar to radar, except that the sensor sends out and receives pulses of light instead of radio waves. Scanning LIDAR systems sweep the environment with a laser beam and measure the distance between the LIDAR output and the point where the laser is reflected. An Optical Phased Array (OPA) can be used for this scanning function, assuring compactness of the optical sensor system [6, 7]. An OPA can be used as an emitter, or as a receiver in a sensor configuration [8]. OPAs can be based on an optical integrated circuit. They allow stable, rapid and precise beam steering without moving parts, contrary to MEMS micro-mirror systems [9], making them robust and insensitive to external constraints such as acceleration. For example, *Quanergy Systems* has announced a long-range solid-state LIDAR sensor system, using an OPA to scan the scene in front of a vehicle [10]. However, today, LIDARs are still expensive and have high power consumption. In OPAs, the beam steering is often achieved using phase shifters where the delay in different optical waveguides is changed via the thermo-optic effect [11] whereas the waveguide effective index change could be induced by applying a mechanical stress using a piezoelectric material [12, 13]. In this paper, we presents such a stress optic modulator using thin-film $Pb(Zr_{0.52},Ti_{0.48})O_3$ (PZT). Firstly, the design and fabrication are detailed. Then characterization results are presented. We used Mach-Zehnder interferometer structures to measure a promising efficiency of the PZT phase shifter of 26V.cm, which is of potential interest for low power optical sensor LIDAR systems.

## II. DESIGN

The monomode optical waveguide was designed to operate in the NIR spectrum (905 nm) at a high power level (>100 mW). Mach Zehnder interferometer structures were used to measure the waveguide phase delay as a function of the voltage applied to the superposed piezoelectric element. We designed a series of Mach-Zehnder interferometers with the PZT elements of lengths, $l_{PZT}$ = 1000, 2000 and 3000 µm, incorporated onto one of the arms above a straight waveguide made in $Si_3N_4$ (see Fig. 1). The distance between the two arms is chosen as being 140µm in order to limit the crosstalk. Grating couplers were added as optical input and outputs for the Mach-Zehnder interferometer system.


Fig. 1. Schematic view of a Mach-Zehnder interferometer, with the PZT actuator incorporated onto one of the arms above a straight waveguide, used to measure the efficiency of a thin-film PZT actuators as a stress-optic modulator.

We designed PZT actuators above the $Si_3N_4$ waveguide using Finite Element Method (FEM) simulations with COMSOL Multiphysics software. We simulate a 50 µm thick 1000×1000 µm² silicon die, considered as infinite (Fig. 2). We fix the mechanical conditions of the backside and the periphery of the die in order to be representative of a silicon substrate. We neglect the top and the bottom electrode due to their low impact on the global mechanical behavior of the stack. The main parameters studied are the optimal thickness (t) of the $SiO_2$ layer between the $Si_3N_4$ waveguide and the PZT actuator, the optimal actuator width (w) and thickness (h).

We simulate an applied electric field through the PZT layer using an actuation voltage of 30 V. Fig. 3 shows the evolution of the Von Mises stress at the center of the $Si_3N_4$ waveguide when the PZT thickness ranges from 0.75 to 2 µm and when the actuator width ranges from 10 to 40 µm. Firstly, we observe that

the stress applied to the waveguide increases linearly with PZT thickness. As already shown in [13], a thicker PZT layer leads to a higher induced mechanical stress. We selected a PZT thickness t = 2 µm due to technological constraints relating to the sol-gel process employed to deposit the PZT material. Then, we observe that the Von Mises stress applied to the $Si_3N_4$ waveguide decreases with respect to the actuator width. As can be seen on Fig. 3b, the Von Mises stress is higher at the edge of the actuator. This results in a Von Mises stress decreasing in the waveguide when the edge of the actuator is farther from the waveguide. We selected an actuator width w of 30 µm.

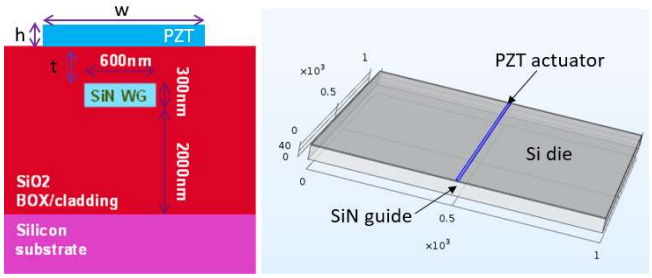


Fig. 2. Schematic cross section of the stack to be optimised showing the main parameters w, t, h and 3D COMSOL Multiphysics model.

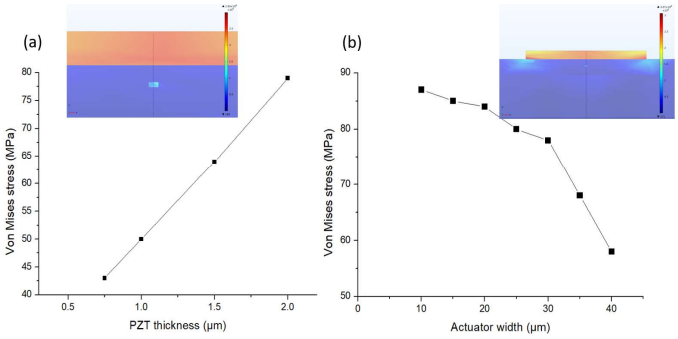


Fig. 3. FEM simualtion of the evolution of the Von Mises stress in the $Si_3N_4$ waveguide as a function of the PZT thickness (a) and the actuator width (b).

Finally, we studied the impact of the $SiO_2$ layer between the $Si_3N_4$ waveguide and the PZT actuator. Fig. 4 shows the Von Mises stress when the silicon oxide thickness ranges from 0.5 to 1.5 µm. We selected the thickness t = 1 µm. This is the optimal value for this configuration (w and h) according to the electromechanical simulations. Moreover, this thickness value will ensure low optical propagation losses.

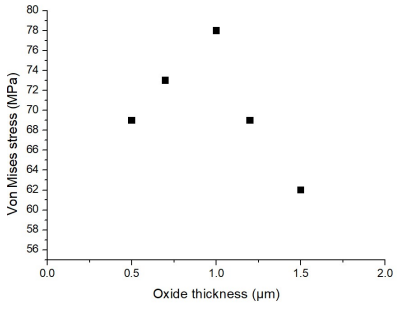


Fig. 4. FEM simulation of the evolution of the Von Mises stress in the $Si_3N_4$ waveguide as a function of the $SiO_2$ layer thickness (t).

## III. TECHNOLOGY

We fabricated the devices on 200 mm silicon wafers. Firstly, a 2µm thick $SiO_2$ layer was deposited on the top of the wafer. The waveguide is based on a 300 nm thick $Si_3N_4$ layer using low-pressure chemical vapor deposition at 750°C. The waveguide is fully etched with a width of 600 nm and is encapsulated by 1 µm of planarised $SiO_2$ using a CMP step. As illustrated in the SEM cross section in Fig. 5, an overpolish of the $SiO_2$ layer led to a thickness of only 0.72 µm, rather than the optimal value of 1 µm. The piezoelectric stack was deposited and etched above the Mach-Zehnder optical structures. This consisted of a 2 µm thick sol-gel PZT layer in between a 100 nm thick bottom electrode and a 100 nm thick Ru top electrode [14, 15]. Then we deposited and patterned a silicon oxide passivation layer followed by gold lines and pads. Fig. 5 gives a schematic cross section of the stack and a SEM cross section of the PZT actuator above the $Si_3N_4$ waveguide. One can note the very dense microstructure of the PZT layer, which indicates the high material quality.

A 200 mm wafer featuring both the $Si_3N_4$ waveguides, and the PZT actuators can be seen in Fig. 6. The inset shows a zoomed image of the PZT actuators above the $Si_3N_4$ waveguides.

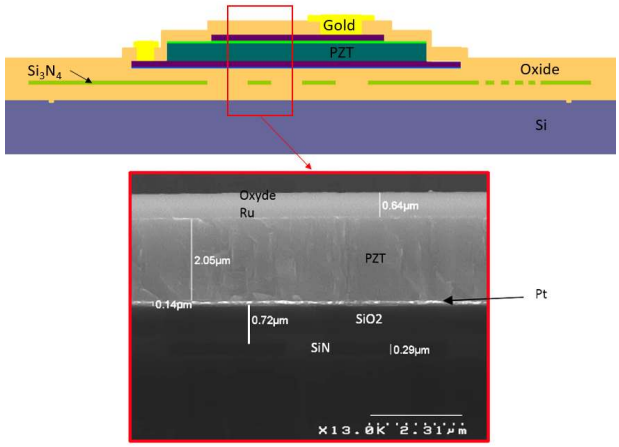


Fig. 5. Schematic and SEM cross section of the PZT actuator above the $Si_3N_4$ waveguide.

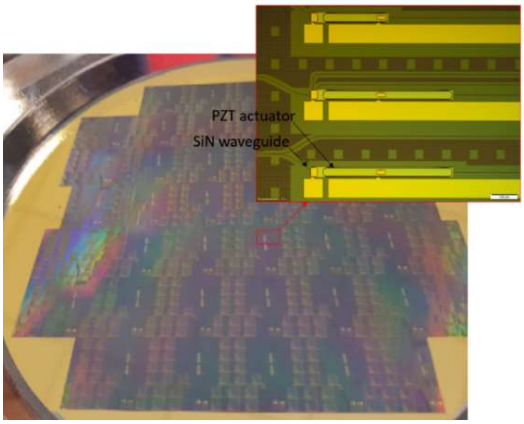


Fig. 6. Photograph of a 8 inch wafer with PZT actuators above the $Si_3N_4$ waveguides and zoomed image of the PZT actuators (inset).

## IV. CHARACTERIZATION

Electrical and optical characterization was performed on the PZT-based stress optic modulator.

### A. Electrical and piezoelectrical characaterizations

Firstly, the ferroelectric, and thus the piezoelectric behavior was confirmed using both capacitance and polarization measurements. Ferroelectric materials, such as PZT, have a very specific polarization curve shape called a ferroelectric hysteresis loop (Fig. 7). From the polarization hysteresis loop, obtained using TF Analyzer 2000 Measurement System from aixACCT, one can extract three important parameters characterizing the polarization abilities of a ferroelectric material, namely coercive voltage $V_c$, remnant polarization $P_r$ and saturated polarization $P_s$. The coercive voltage is the voltage at zero polarization. The remnant polarization is the polarization at zero voltage and the saturated polarization is the maximum or minimum polarization. From Fig. 7, we can extract respectively $V_c$ = 7.5 V, $P_r$=27µC/cm² and $P_s$ = 52 µC/cm². These values are in line with the expected values.

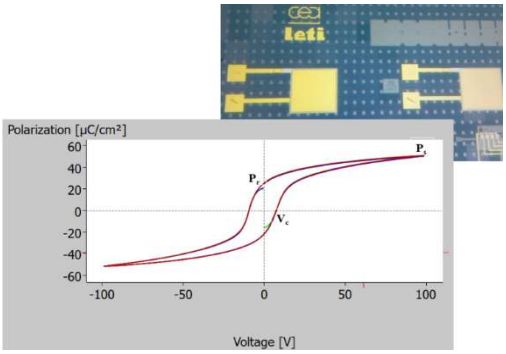


Fig. 7. PV loops measured on a PZT 5×5 mm² capacitance.

We also measured the capacitance of PZT actuators using a HP 4194A Impedance Analyzer. From these measurements, we can estimate the maximum relative permittivity of the PZT material as being 1450, which is in line with the expected value.

### B. Optical measurements

In order to characterize the optical performance of the PZT phase shifter, we used a series of Mach-Zehnder interferometers with the PZT element of lengths, $l_{PZT}$ = 1000, 2000 and 3000 µm, incorporated onto one of the arms above a straight waveguide (see Fig. 1). We then measured the optical transmission of the test structure at a wavelength of 905 nm and as a function of the voltage applied to the PZT element. Fig. 8a shows this variation in transmission as a function of the voltage applied to the PZT. A maximum in the transmission indicates constructive interference at the waveguide combiner at the interferometer output. A transmission minimum indicates destructive interference. We can therefore infer that the voltage difference to pass from a maximum to a minimum is that required for a 180° phase shift in the waveguide. We see that in the range of voltage considered, a 180° phase shift was only possible for the structures with $L_{PZT}$ = 2000 and 3000 µm. For the 3000 µm PZT, we measure Vπ = 65 V (indicated in Fig. 8a) and for the 2000 µm element, Vπ is close to 130 V. The efficiency of the PZT phase shifter is therefore $V\pi L\pi \approx$ 20-26 V.cm. The energy dissipation of the actuator, considered as a parallel plate capacitor can be estimated roughly as being 800 nW per π phase shift. It proves the low power potential of the PZT phase shifter compared to thermo-optic modulators that typically consume approximatively 200-500 mW [13]. Fig. 8b shows the optical losses as a function of applied PZT voltage for the different PZT element lengths. It can be seen that the proximity of the bottom metal PZT contact leads to optical losses that increase with the PZT length, but are constant as a function of the applied PZT voltage. This is a consequence of the previously mentioned over polish of the $SiO_2$ waveguide cladding layer. Since the optical losses decline exponentially as the distance between the waveguide and the metal increases, a target cladding thickness of 1 µm (rather than the fabricated thickness of 0.72 µm) would probably eliminate these losses.

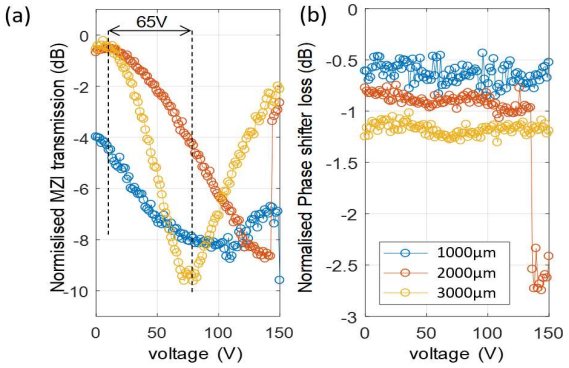


Fig. 8. (a)- Measurement of the optical transmission at a wavelength of 905nm of the test structure as a function of the voltage applied to the PZT element. (b)- Optical losses as a function of applied PZT voltage for the different PZT element lengths.

## V. CONCLUSION

We present a stress optic modulator using PZT actuators, with potential to be implemented in a solid-state optical sensor LIDAR system. Design optimization was performed using FEM simulation, and demonstrators were fabricated using standard processes on 200 mm silicon wafers. Using electrical characterization, we extracted PZT characteristics in line with the expected values and proved the functionality of the PZT actuators. Then optical characterization shows the efficiency of the PZT phase shifter as being $V\pi L\pi$ = 20-26 V.cm, with a low energy dissipation of 800 nW per π phase shift. The measured optical losses are very likely due to the unintentionally reduced $SiO_2$ encapsulation layer above the waveguides. Achieving the nominal thickness of 1 µm would probably eliminate the measured optical propagation losses and would also be further optimize the PZT actuator functionality. These promising results potentially open an alternative path for low power solid-state LIDAR systems.

## ACKNOWLEDGMENT

The authors wish to acknowledge all participants at the DEMO3S (Distance, Events, Motion, by Optical Sensors for a Safer Society) project for their participation in these developments.

## REFERENCES


[1] B. Schwarz, "LIDAR: Mapping the world in 3D", Nature Photonics, vol. 4, July 2010, pp. 429-430.

[2] I.H. Park, JA. Jeon, J. Nam, S. Nam, J. Lee, JH. Park, J. Yang, T. Ebisuzaki, Y. Kawasaki, Y. Takizawa and S. Wada, "A New LIDAR Method using MEMS Micromirror Array for the JEM-EUSO mission", in Proc. Of the 31st ICRC Conference, 2009.

[3] D. Göhring, M. Wang, M. Schnürmacher and T. Ganjineh, "Radar/LIDAR sensor fusion for car-following on highways", Proc. Of the 5th Int. Conf. on Automation, Robotics and Applications, 2011, pp. 407-412.

[4] J. Wei, JM. Snider, J. Kim, JM. Dolan, R. Rajkumar and B. Litouhi, "Towards a viable autonomous driving research platform", IEEE Intelligent Vehicles Symposium (IV), June 23-26, 2013, pp. 763-770.

[5] AY. Hata and DF. Wolf, "Feature detection for vehicle localization in urban environments using a multilayer LIDAR", IEEE Transactions on Intelligent Transportation Systems, vol. 17, n° 2, February 2016, pp. 420-429.

[6] Christopher V. Poulton, Peter Russo, Erman Timurdogan, Michael Whitson, Matthew J. Byrd, Ehsan Hosseini, Benjamin Moss, Zhan Su, Diedrik Vermeulen, and Michael R. Watts, "High-Performance Integrated Optical Phased Arrays for Chip-Scale Beam Steering and LiDAR", Conference on Lasers and Electro-Optics (CLEO: Applications and Technology), 2018, paper ATu3R.2.

[7] S.Amoruso, A.Amodeo, M.Armenante, A.Boselli, L.Mona, M.Pandolfi, G.Pappalardo, R.Velotta, N.Spinelli, and X.Wang, "Development of a tunable IR lidar system", Optics and Lasers en Engineering, vol. 37, Issue 5, May 2002, pp. 521-532.

[8] R. Fatemi, B. Abiri, A. Khachaturian and A. Hajimiri, "High sensitivity active flat optics optical phased array receiver with a two-dimensional aperture", Optics Express, vol. 26, Issue 23, 2018, pp. 29983–29999.

[9] F. Casset, P. Poncet, B. Desloges, F. Domingues Dos Santos, JS. Danel, S. Fanget, "Resonant asymmetric micro-mirror using Electro Active Polymer actuators", Proc. of the 17th IEEE Conference on Sensors (IEEE Sensors), 2018, pp. 271-274.

[10] E. Ackerman, "Quanergy Announces $250 Solid-State LIDAR for Cars, Robots, and More", in IEEE Spectrum, 7 January 2016.

[11] NA. Tyler, D. Fowler, S. Malhouitre, S. Garcia, P. Grosse, W. Rabaud and B. Szelag, "SiN integrated optical phased arrays for two-dimensional beam steering at a single near-infrared wavelength," Optics Express, vol. 27, no. 4, Feb. 2019, p. 5851.

[12] JP. Epping, D. Marchenko, A. Leinse, R. Mateman, M. Hoeman, L. Weres, EJ. Klein, CGH. Roeleffzen, M. Dekkers and RG. Heideman, "Ultra-low-power stress-optics modulator for microwave photonics", in Procs of SPIE, Integrated Optics: Devices, Materials, and Technologies XXI, vol. 10106, 2017, pp. 101060F1-101060F8.

[13] N. Hosseini, R. Dekker, M. Hoekman, M. Dekkers, J. Bos, A. Leinse and R. Heideman, "Stress-optic modulator in TriPleX platform using a piezoelectric lead zirconate titanate (PZT) thin-film", Optivs Express, vol. 23, n° 11, 1 June 2015, pp. 14018-14026.

[14] E. Defaÿ, Integration of ferroelectric and piezoelectric thin films, Wiley, 2011.

[15] M. Cueff, M. Allain, J. Abergel, G. Le Rhun, M. Aïd, D. Faralli, E. Defaÿ, "Influence of the crystallographic orientation of Pb(Zr,Ti)O3 films on the transverse piezoelectric coefficient d31", IEEE Int. Ultrasonics Conference, October 18-21, 2011, pp. 1948-1951.